Computer robust parameter design of surface eddy current probes. Developing software design of numerical experiments creating ⋆

Volodymyr Halchenko[1,†], Ruslana Trembovetska[1,†] and Volodymyr Tychkov[1*,†]

[1] *Cherkasy State Technological University, 460 Shevchenko Blvd., Cherkasy, 18006, Ukraine*

Abstract

In this study, the initial stage of computer robust parameter design of a surface eddy-current probe on the example of a thickness gauge was performed using the integration of the Taguchi method with numerical modeling. It involves the selection of controllable design and operating parameters of the probe and uncontrollable noise parameters. The software for calculating the output signal of the thickness gauge was created and verified. In order to establish the boundary values of the factors, numerical modeling was performed, which allowed to obtain graphical dependencies of the change in the output signal of the probe on the variation of the selected factors. Based on the orthogonal arrays, taking into account the selected factors, a design of numerical experiments was created that allows creating robust parameter design using the developed software. Without eliminating the real causes of interference in the formation of the probe output signal, it ensures the selection of a rational variant of the set of its design and operating parameters, which implements the minimum variability of the probe response to noise factors at the initial design stage.

Keywords

computer robust parameter design, Taguchi's complex method, orthogonal array, numerical experiments design, eddy current probe

1. Introduction

It is a well-known fact that the use of eddy current probes (ECPs), in particular, surface ones, in non-destructive testing is based on the multiparameter nature of the information to be selected. This provides many opportunities for measuring a significant number of information parameters.

However, determining one of the specific controllable parameters leads to problems associated with overcoming the influence of uncontrollable ones, which also form the output signal of the probes and are essentially noise. Therefore, ECPs can be used for various purposes as part of flaw detection material integrity violations in the testing objects (TO) [1]; in

⋆ITTAP'2024: 4th International Workshop on Information Technologies: Theoretical and Applied Problems, November 20–22, 2024, Ternopil, Ukraine, Opole, Poland

1* Corresponding author.

† These authors contributed equally.

v.halchenko@chdtu.edu.ua (V. Ya. Halchenko); r.trembovetska@chdtu.edu.ua (R. V. Trembovetska); v.tychkov@chdtu.edu.ua (V. V. Tychkov)

0000-0003-0304-372X (V. Ya. Halchenko); 0000-0002-2308-6690 (R. V. Trembovetska); 0000-0001-9997-307X (V. V. Tychkov)

structuroscopes - to determine the structural state of the TO as a result of fixing the depth profiling of electrical conductivity and/or magnetic permeability [2, 3], in controlling mechanical stresses [4], chemical composition, quality of technological processing of parts by chemical and physical methods, and structural anomalies; in thickness gauges - to control the geometric dimensions of the TO [5] and the coatings' thickness [6, 7].

Depending on the intended purpose of the measurement, in each of the above cases of ECP application, the above-mentioned factors perform different functions from assisting to hindering, they were constantly exchanging roles. Each of these examples involves the use of special techniques and methods for suppressing noise signals, which are often based on the analysis of the dependence of the ECP output signal on a number of factors, with an attempt to separate their influence [1, 2, 3], but this approach is quite difficult to implement if it is necessary to suppress more than one of them. Other methods of the same purpose are known, which are used either separately or in combination, in particular, stabilization of testing conditions, application of spectral analysis, etc. However, these techniques for selecting useful information from the ECP signal are either not fully perfect or rather complicated in practical implementation, which does not add to their effectiveness. This is especially true in multiparameter measurement cases.

Thus, the noted limitations of selecting useful information from the ECP necessitate the search for other approaches to solving this problem that would provide an increased signal-to-noise ratio (SNR). Recently, the method of robust parameter design [8, 9] has become quite popular among researchers, which has attained wide application in various fields of instrumentation and measurement technology. The point is that this effect can be achieved at the initial stage of ECP computer design, and not during the selection and processing of the probe signal. The ECP measurement process is characterized by uncertainties such as changes in the lift-off, local changes in the electrophysical properties of the material, local variations in the geometry of the TO, possible imperfections of its surface, such as roughness, curvature, etc. In such conditions, the robust parameter design of the ECP provides maximum sensitivity to the controllable parameter, while for other influential, but interfering with measurements, the sensitivity is minimal. Therefore, robust parameter design can be used to effectively select rational design and operating parameters of the ECP, which provide the probes with resistance to noise caused by uncontrollable variations, i.e., robustification is aimed at numerical finding parameters of controllable factors that minimize the deviation of the response from uncontrollable ones due to the use of nonlinearity of their effect on the signal by computing facilities. Robust parameter design is usually based on experimental data, but it can also be obtained by computer modeling as a result of numerical experiments, and therefore is an engineering methodology. Its result is achieved by reducing the effects of variations without actually eliminating their causes. A numerical indicator of successful robustification in accordance with the proposed design computer concept can be considered a criterion that requires maximization (quality loss function “larger-the better”) by the choice of factor levels [10] and ensures the largest value of the ECP signal and minimization of its variability, i.e., variance, and corresponds to the expression:

$$\frac{S}{N}\text{ratio} = -10 \cdot \log_{10} \frac{1}{n} \cdot \sum_{i=1}^{n} \frac{1}{E_i^2}, \quad (1)$$

where n is the sample size, E is the ECP signal.

Despite the widespread use of robust parameter design based on the Taguchi method in various fields of science and technology, as evidenced by quite old publications, in particular [11], the authors have not found any studies on its application in the design of ECPs. At the same time, the relevance of the results of its use has not been lost in the present, as evidenced, for example, by articles [12, 13, 14]. Significant practical results of its application with the involvement of insignificant computational resources and the absence of interventions to level the effect of noise factors are undeniable.

Thus, the **purpose** of the article is to create a methodology for computer robust parameter design of surface eddy current probes and related software based on the integration of the Taguchi method and numerical modeling, which allows, at the initial stage of choosing its design, to achieve selective adjustment of the probes` sensitivity to measure the useful signal while reducing it to uncontrollable interfering factors.

2. Research methodology

In order to implement computer robust parameter design of the ECP, a number of steps are required according to the Taguchi method. A general scheme illustrating the entire design process is shown in Fig. 1.

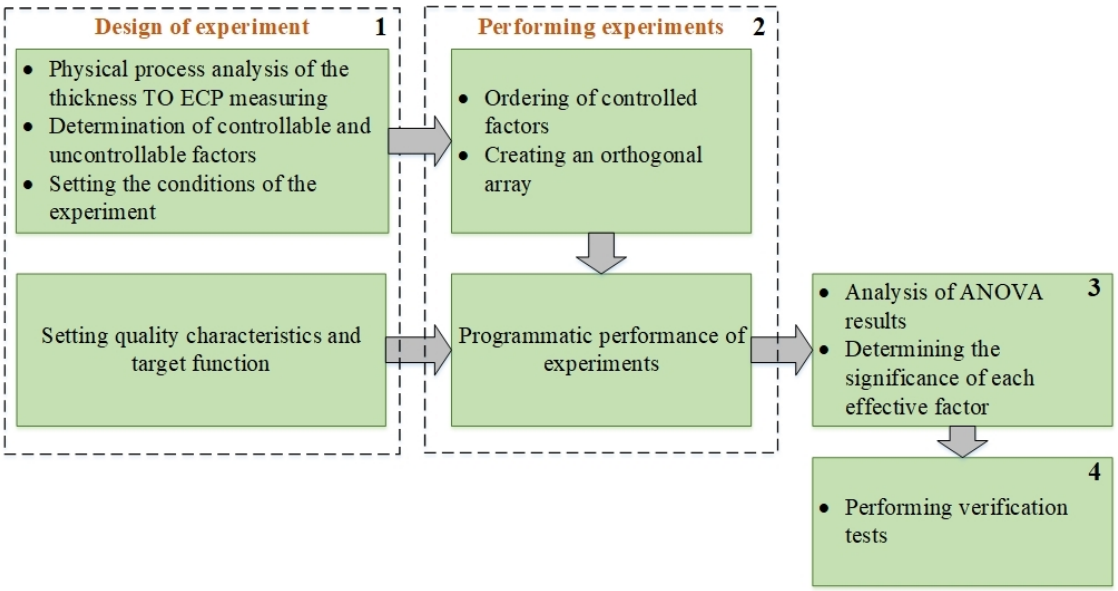

Figure 1: General scheme of the robust parameter design process of the ECP.

The Taguchi method uses special orthogonal arrays to design of experiment and analyze the resulting data using the SNR. For further implementation of this algorithm, a thorough understanding of the measuring process, for example of the TO's thickness, which, from the general view shown in Fig. 2 a, should be interpreted in the appropriate terms of eddy current determination of the signal parameter (Fig. 2 b).

understand the relationship observed between the input measured parameter and the target characteristic of the SNR ECP, taking into account the influence of controllable, i.e., design and operating factors, and uncontrollable, i.e., noise sources. The input signal is subject to changes with the corresponding observation of the output response, which allows us to investigate the value of the controllable factors, the combination of which ensures the smallest possible variability of the output response.

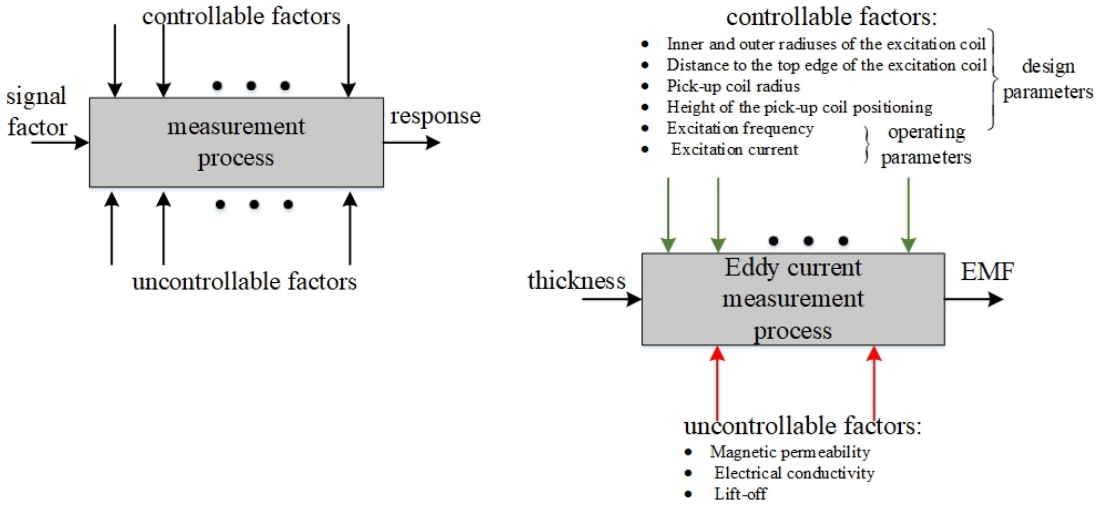

Figure 2: Measurement process: a - in the general case; b - by eddy current probe.

Computer modeling is used in these studies to create numerical design of experiments.

The electrodynamic mathematical model for a coil with an alternating sinusoidal current $\dot{I} = Ie^{j\omega t}$

of angular frequency ω, which describes the process of eddy current measurement by a surface probe over an TO in the form of a conductive plate of finite thickness (Fig. 3), was obtained as a result of analytical solution of the partial differential boundary value problem in the cylindrical coordinate system [15]:

$$\frac{1}{\rho}\cdot\frac{\partial}{\partial\rho}\left(\rho\cdot\frac{\partial\dot{A}}{\partial\rho}\right)+\frac{\partial^2\dot{A}}{\partial z^2}-\left(\frac{1}{\rho}-k^2\right)\cdot\dot{A}=-\mu\cdot\mu_o\cdot j_{ex}$$
$$k^2=-j\cdot\mu_0\cdot\mu\cdot\sigma \qquad (2)$$

,

$\dot{A}$

where - is the azimuthal component of the magnetic vector potential, Wb/m; ρ, z – coordinates, m; μ0 = 4·π·10-7 is the magnetic constant in vacuum, H/m; μ - is the relative magnetic permeability of the medium; jex - density of currents of external sources, A/m2; σ - is the electrical conductivity of the medium, S/m.

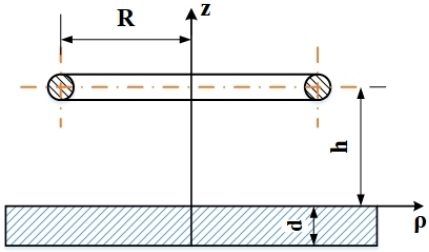

Figure 3: Geometric model of the eddy current measurement process.

Equation (1) was solved on the following boundary conditions:

$$\dot{A}_p(\rho,z)\Big|_{z=z_p} = \dot{A}_{p+1}(\rho,z)\Big|_{z=z_p}$$
$$\frac{1}{\mu_p}\cdot\frac{\partial\dot{A}_p}{\partial z}\Big|_{z=z_p} = \frac{1}{\mu_{p+1}}\cdot\frac{\partial\dot{A}_{p+1}}{\partial z}\Big|_{z=z_p} \quad (3)$$

,

where p is the number of the boundary of media distribution, p = 1, 2.

The solution was found through the following assumptions: the probe field is considered quasi-stationary; wave processes in the air are neglected; bias currents in the conductive medium are also neglected; the diameter of the coil cross-section is considered very small. Under these conditions, the magnetic vector potential in the area of the ECP pick-up coil can be determined by the formula:

$$\dot{A}_1 = \frac{\mu_0\cdot R\cdot\dot{I}}{2}\left[\int_0^\infty J_1(\lambda R)\cdot J_1(\lambda\rho)\cdot e^{-\lambda|z-h|}d\lambda + \int_0^\infty J_1(\lambda R)\cdot J_1(\lambda\rho)\cdot\varphi_1\cdot e^{-\lambda(z+h)}d\lambda\right] \quad (4)$$

,

$$\varphi_1 = \frac{(\lambda\mu_2 - q_2)\cdot(\mu_3 q_2 + \mu_2 q_3)\cdot e^{dq_2} - (\lambda\mu_2 + q_2)\cdot(\mu_2 q_3 - \mu_3 q_2)\cdot e^{-dq_2}}{\Lambda},$$

where

$$\Lambda = (\lambda\mu_2 + q_2)\cdot(\mu_2 q_3 + \mu_3 q_2)\cdot e^{dq_2} - (\lambda\mu_2 - q_2)\cdot(\mu_2 q_3 - \mu_3 q_2)\cdot e^{-dq_2},$$

$$q_2 = \sqrt{\lambda^2 - k_2^2} = \sqrt{\lambda^2 + j\cdot\omega\cdot\sigma_2\cdot\mu_0\cdot\mu_2},\ q_3 = \sqrt{\lambda^2 - k_3^2} = \sqrt{\lambda^2 + j\cdot\omega\cdot\sigma_3\cdot\mu_0\cdot\mu_3},\ \mu_3 = 1,\ \sigma_3 = 0,$$

J1() is a first-order Bessel function of the first kind.

If we assume that the real ECP excitation coil has finite geometric dimensions, then to take into account its cross-section (R2-R1)⋄(h2-h1), the formula for calculating the magnetic vector potential will be found by integration according to the expression:

$$\dot{A} = \left[\frac{1}{(R2 - R1) \cdot (h2 - h1)} \right] \int_{h1}^{h2} \int_{R1}^{R2} \dot{A}_1 dR dh. \quad (5)$$

Thus, the output signal of the surface ECP in the form of an EMF induced in the pick-up coil can be calculated according to the formula:

$$E = -j \cdot \omega \cdot w_{mes} \cdot \oint_{Lc} \dot{A}(P) dl_p \quad (6)$$

,

where wmes is the number of turns of the pick-up coil; P is the observation point with coordinates (ρ, z) belonging to the contour Lc of the pick-up coil.

To calculate the non-proprietary integral of the first kind (4), it makes sense to use the Gauss-Laguerre quadrature formula. The creation of the design of experiment involves the calculation of the ECP EMF for numerical modeling of the measurement process, for which the corresponding software was developed in the PTC MathCAD Prime environment. Its verification for the case of representing the probe excitation system by a coil (4) was carried out in the software environment for solving and simulating various engineering applications COMSOL Multiphysics using the finite element method. The grid model for this numerical experiment is shown in Fig. 4, and Fig. 5 shows the results of calculations of the vector magnetic potential performed at a set of observation points.

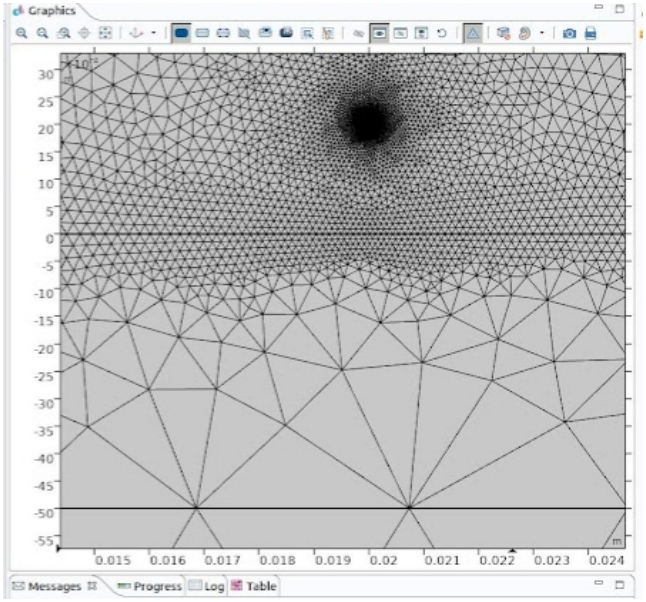

Figure 4: Grid model of the surface ECP

The test numerical simulation was performed with the following input data: (ρ, z) = (10·10-3, 1·10-3) m; f = 2 kHz; d = 5·10-3 m; R = 20·10-3 m; h = 2·10-3 m; I = 1 A; ? = 3.77·107 S/m, μ = 1. Comparison of the results of calculating the values of the vector potential obtained in the

COMSOL Multiphysics environment (Fig. 5) and in the PTC MathCAD Prime environment according to formula (4) gives a coincidence of the vector potential values with an accuracy of 0.039 %, which indicates the adequacy of the created software for modeling of the measurement process.

Consequently, it becomes possible to set the lower and upper limits of variation of all influencing factors by modeling, that is, to fulfill the task of block 1 of the general scheme of the robust parameter design process of the ECP. This, in turn, allows choosing the type of orthogonal array and complete the creation of numerical design of experiments for further computer robust parameter design.

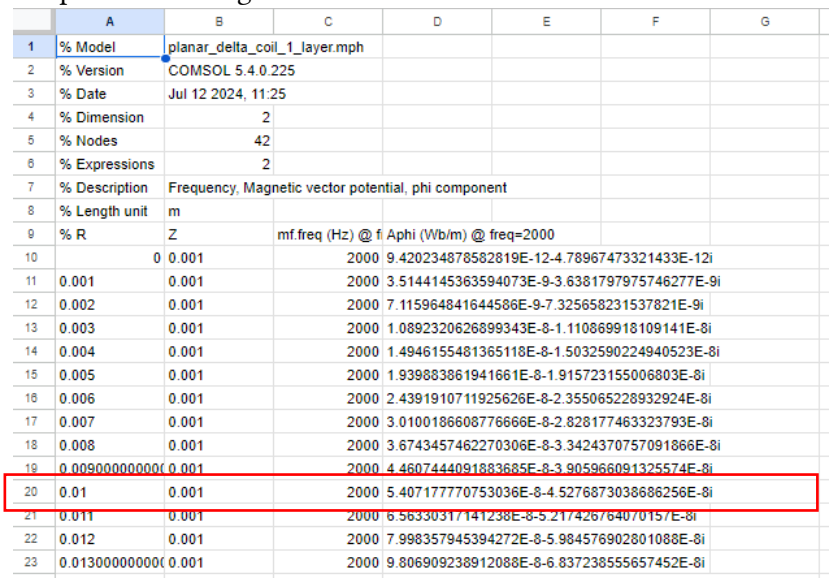

	A	B	C	D	E	F	G
1	% Model	planar_delta_coil_1_layer.mph					
2	% Version	COMSOL 5.4.0.225					
3	% Date	Jul 12 2024, 11:25					
4	% Dimension	2					
5	% Nodes	42					
6	% Expressions	2					
7	% Description	Frequency, Magnetic vector potential, phi component					
8	% Length unit	m					
9	% R	Z	mf.freq (Hz) @ fi	Aphi (Wb/m) @ freq=2000			
10	0	0.001	2000	9.420234878582819E-12-4.78967473321433E-12i			
11	0.001	0.001	2000	3.5144145363594073E-9-3.6381797975746277E-9i			
12	0.002	0.001	2000	7.115964841644586E-9-7.325658231537821E-9i			
13	0.003	0.001	2000	1.0892320626899343E-8-1.110869918109141E-8i			
14	0.004	0.001	2000	1.4946155481365118E-8-1.5032590224940523E-8i			
15	0.005	0.001	2000	1.939883861941661E-8-1.915723155006803E-8i			
16	0.006	0.001	2000	2.4391910711925626E-8-2.355065228932924E-8i			
17	0.007	0.001	2000	3.0100186608776666E-8-2.828177463323793E-8i			
18	0.008	0.001	2000	3.6743457462270306E-8-3.3424370757091866E-8i			
19	0.009000000000(	0.001	2000	4.4607444091883685E-8-3.905966091325574E-8i			
20	0.01	0.001	2000	5.407177770753036E-8-4.5276873038686256E-8i			
21	0.011	0.001	2000	6.5633031714123 8E-8-5.217426764070157E-8i			
22	0.012	0.001	2000	7.998357945394272E-8-5.984576902801088E-8i			
23	0.013000000000(	0.001	2000	9.806909238912088E-8-6.837238555657452E-8i			

Figure 5: Results of test calculations of the vector magnetic potential.

3. Numerical experiments

For the purpose of further research, we will limit ourselves to considering the example of an eddy current thickness gauge, while similar actions are assumed for other measurements. The analysis of the physical process of thickness measuring of the TO of the ECP allows to identify the following influencing factors on the output signal of the probe, including controllable (C), noise (N), or uncontrollable and signal (S) (Table 1).

Table 1
Influencing factors on the output signal of the ECP during thickness measurement of the testing object

Factor	Type of factor	Type of parameter
Internal radius of the excitation coil R1	C	
External radius of the excitation coil R2	C	
Radius of the pick-up coil ρ	C	Structural
Height of the pick-up coil z	C	
Distance to the top edge of the excitation coil h2	C	
Excitation frequency f	C	Mode
Excitation current I	C	
Magnetic permeability μ	N	
Electrical conductivity σ	N	Noise
Lift-off h1	N	
TO thickness d	S	Signal

Subsequently, to establish the sensitivity of the probe to measuring the useful signal, a series of numerical experiments were performed to determine the dependence of the ECP output signal on the influencing factors using formula (6). In this case, in each individual experiment, the factor under analysis varied within certain specified limits, while all other factors remained unchanged, i.e. fixed. The initial data for this analysis are as follows: R1=20·10-3 m, R2=21·10-3 m, h1=2·10-3 m, h2=3·10-3 m, z=1·10-3 m, r=13·10-3 m, d=3·10-3 m, f=1.5 kHz, I=1 A, σ=6.99·106 S/m, μ=20.

Fig. 6 shows the graphs of changes in the ECP signals when varying such design parameters as the internal R1 and external R2 radii of the excitation coil. In this case, taking into account the initial input data, the variation of the inner radius is set in the range $R1-0.08\cdot R1 \le R1 \le R1+0.04\cdot R1$, and the outer radius $R2-0.004\cdot R2 \le R2 \le R2+0.12\cdot R2$ respectively.

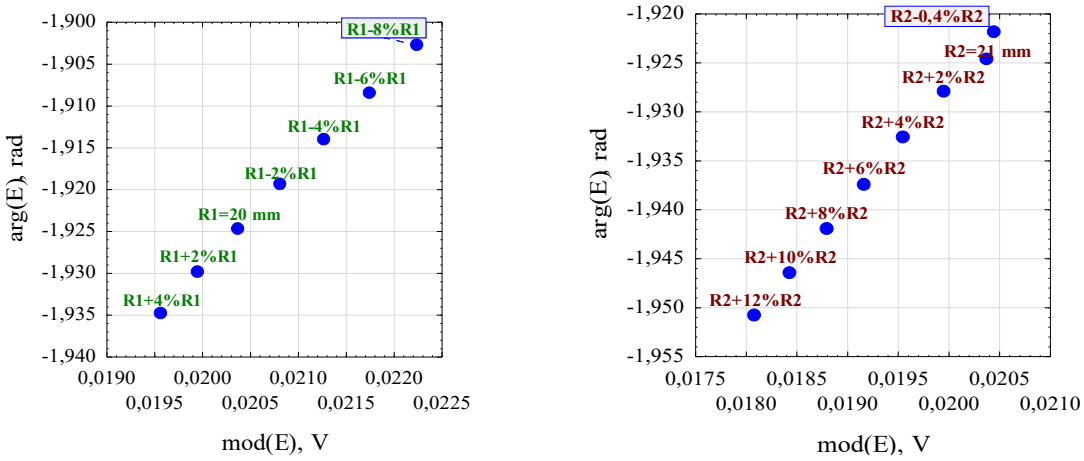

Figure 6: Output signal of the eddy current thickness gauge when changing the design parameters: a - inner radius of the excitation coil R1; b - outer radius of the excitation coil R2.

Figure 7 shows the dependence of the probe signal on the change in the height of the pick-up coil z and its radius ρ.

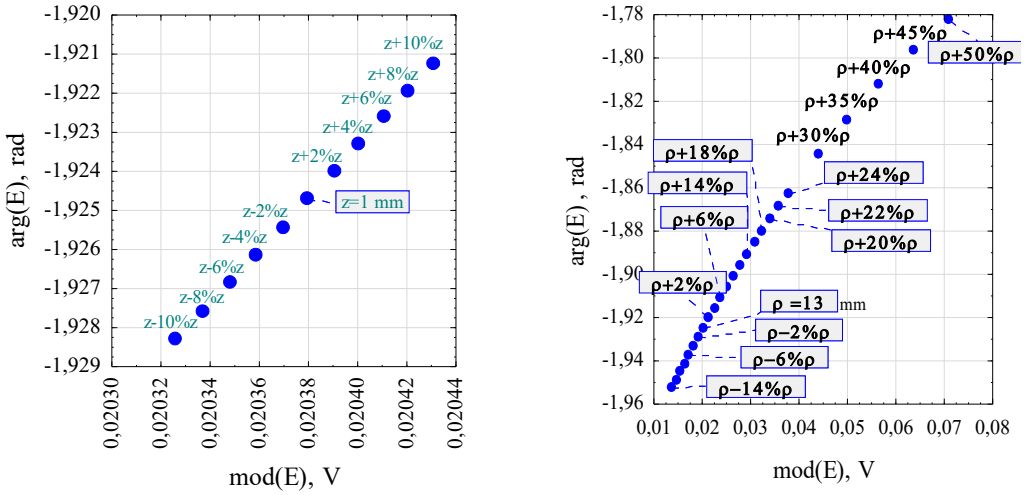

Figure 7: Dependence of the probe output signal on the change in the design parameters of the pick-up coil: a - height z; b - radius ρ.

The next design parameter, namely the lift-off h1, was set within $h1 - 0.08 \cdot h1 \le h1 \le h1 + 0.08 \cdot h1$, while simultaneously ensuring the condition of constancy of the coil cross-sectional area (h2-h1=const). The variation of the ECP signal from the variation of the lift-off h1 and the distance to the upper edge of the excitation coil h2 and the thickness of the TO d is shown in Fig. 8.

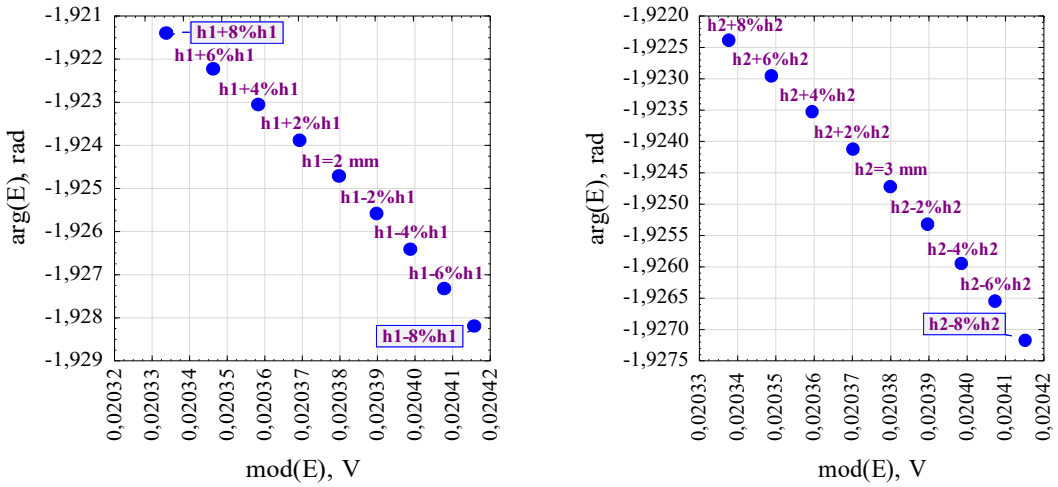

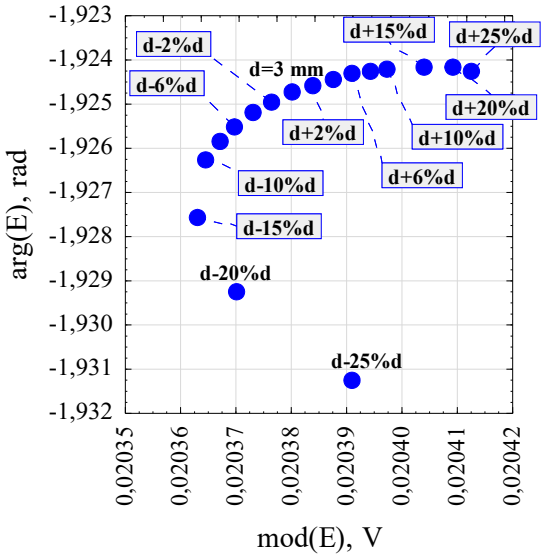

Figure 8: Dependence of the output signal of the eddy current thickness gauge on changes in the parameters: a - lift-off h1; b - distance to the upper edge of the excitation coil h2; c - thickness of the TO d.

The following graph (Fig. 9) demonstrates the dependence of the output signal of the probe on changes in uncontrollable factors, in particular, the magnetic permeability and electrical conductivity of the TO.

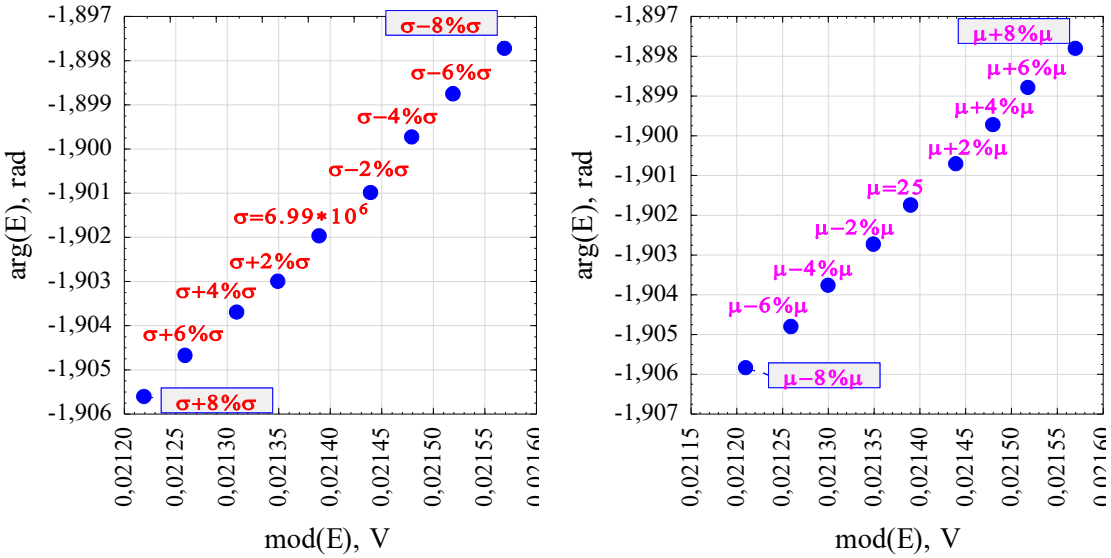

Figure 9: Output signal of the eddy current thickness gauge when changing uncontrolled factors: a - electrical conductivity σ; b - magnetic permeability μ.

In conclusion, we studied the change in the ECP signal to varying the operating parameters of the excitation coil and illustrated the results obtained (Fig. 10).

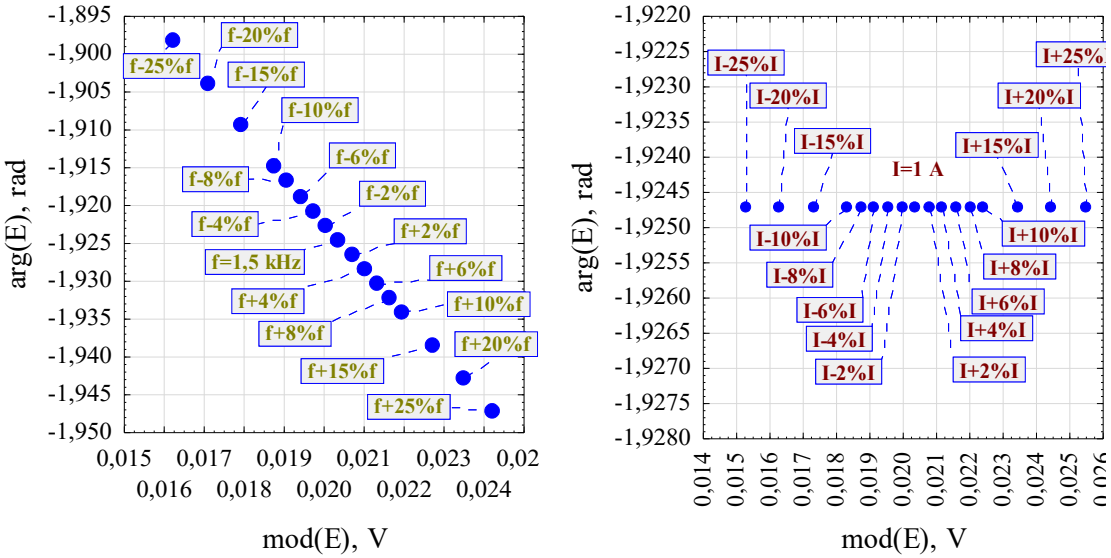

Figure 10: Output signal of the eddy current thickness gauge when varying the operating parameters of the excitation coil: a - frequency f; b - current I.

Based on the obtained graphs (Fig. 6 - Fig. 10), it is possible to numerically determine the sensitivity of the ECP and determine, respectively, the lower and upper limits of change of each influencing factor.

Thus, the numerical values of the limits of change of the factors, finally determined by the graphs, are shown in Table 2.

Table 2

Influencing factors on the output signal of the ECP when measuring the thickness of the TO

Limits of change of influencing factors	Lower bound	Upper bound	Factor symbol
Inner radius of the excitation coil R1, m	0.0184	0.0208	A
Outer radius of the excitation coil R2, m	0.020916	0.02352	B
Radius of the pick-up coil ρ, m	0.01118	0.0195	C
Distance to the top edge of the excitation coil h2, m	2.76·10-3	3.24·10-3	D
Height of the pick-up coil z, m	9·10-4	1.1·10-3	E
Excitation frequency f, kHz	1.125·103	1.875·103	F
Excitation current I, A	0.75	1.25	G
Magnetic permeability μ	18.4	21.6	H
Electrical conductivity σ, S/m	6.431·106	7.549·106	J
Lift-off h1, m	1.84·10-3	2.16·10-3	K

The orthogonal array L18(21,37) was chosen for the controllable factors, and the array L9(34) for the uncontrollable ones with three levels of gradation for both types (Table 3) [16, 17]. Subsequently, modernized orthogonal arrays were used, in which one factor was removed, in particular, a factor with two gradations was removed in L18(21,37), and one extra factor was removed in L9(34). The values of the factors in the selected orthogonal arrays are converted into units of real physical quantities (Table 4), corresponding to low, medium, and high levels. The total amount of computational experiments to be performed according to this design is obtained by combining the arrays L18(21,37) and L9(34), i.e., 18·9=162. Thus, for each experiment, the EMF of the probe is determined at the specified settings for each level of all factors.

Table 3

Orthogonal arrays $L_{18}(2^1,3^7)$ for controllable and $L_9(3^4)$ for uncontrollable factors

№	Factor controllable							Factor uncontrollable		
experiment	**A**	**B**	**C**	**D**	**E**	**F**	**G**	**H**	**J**	**K**
1	1	1	1	1	1	1	1	1	1	1
2	1	2	2	2	2	2	2	1	2	2
3	1	3	3	3	3	3	3	1	3	3
4	2	1	1	2	2	3	3	2	1	1
5	2	2	2	3	3	1	1	2	2	2
6	2	3	3	1	1	2	2	2	3	3
7	3	1	2	1	3	2	3	3	1	2
8	3	2	3	2	1	3	1	3	2	3
9	3	3	1	3	2	1	2	3	3	1
10	1	1	3	3	2	2	1			
11	1	2	1	1	3	3	2			
12	1	3	2	2	1	1	3			
13	2	1	2	3	1	3	2			
14	2	2	3	1	2	1	3			
15	2	3	1	2	3	2	1			
16	3	1	3	2	3	1	2			
17	3	2	1	3	1	2	3			
18	3	3	2	1	2	3	1			

Table 4

Design of experiment according to Taguchi method

№	Factor controllable						
	A	**B**	**C**	**D**	**E**	**F**	**G**
1	0.0184	0.020916	0.01118	0.00276	0.0009	1125	0.75
2	0.0184	0.022218	0.01534	0.003	0.001	1500	1
3	0.0184	0.02352	0.0195	0.00324	0.0011	1875	1.25
4	0.0196	0.020916	0.01118	0.003	0.001	1875	1.25
5	0.0196	0.022218	0.01534	0.00324	0.0011	1125	0.75
6	0.0196	0.02352	0.0195	0.00276	0.0009	1500	1
7	0.0208	0.020916	0.01534	0.00276	0.0011	1500	1.25

8	0.0208	0.022218	0.0195	0.003	0.0009	1875	0.75
9	0.0208	0.02352	0.01118	0.00324	0.001	1125	1
10	0.0184	0.020916	0.0195	0.00324	0.001	1500	0.75
11	0.0184	0.022218	0.01118	0.00276	0.0011	1875	1
12	0.0184	0.02352	0.01534	0.003	0.0009	1125	1.25
13	0.0196	0.020916	0.01534	0.00324	0.0009	1875	1
14	0.0196	0.022218	0.0195	0.00276	0.001	1125	1.25
15	0.0196	0.02352	0.01118	0.003	0.0011	1500	0.75
16	0.0208	0.020916	0.0195	0.003	0.0011	1125	1
17	0.0208	0.022218	0.01118	0.00324	0.0009	1500	1.25
18	0.0208	0.02352	0.01534	0.00276	0.001	1875	0.75

Table 5
Design of experiment according to Taguchi method

№	Factor uncontrollable		
	H	**J**	**K**
1	18.4	6431000	0.00184
2	18.4	6990000	0.002
3	18.4	7549000	0.00216
4	20	6431000	0.002
5	20	6990000	0.00216
6	20	7549000	0.00184
7	21.6	6431000	0.00216
8	21.6	6990000	0.00184
9	21.6	7549000	0.002

Thus, the obtained numerical design of experiments allows for computer robust parameter design of the eddy current thickness gauge by selecting rational combinations of the probe's design and operating parameters. The design quality largely determines the effectiveness of the ECP design, which has already been proven by the authors' personal experience in applying other similar data-driven design methods that use designs of experiment [18, 19].

4. Conclusion

Thus, the study carried out, using the example of a thickness gauge, the initial stage of computer robust parameter design of a surface eddy current probe based on an integrated approach of combining numerical modeling with the Taguchi method. The physical process of thickness measurement by the probe is analyzed and, as a result, their controllable and uncontrollable factors are identified from all possible influencing factors.

Graphs of the output signals of the ECP before changing the parameters of the influencing factors were obtained and their lower and upper limits were determined, respectively. Taking into account the number of relevant factors, two types of orthogonal arrays were selected, namely $L_{18}(2^1,3^7)$ and $L_9(3^4)$ with three levels of their gradation.

The software for the implementation of computer robust parameter design of surface ECP was created, and its verification in the COMSOL Multiphysics environment for calculating the ECP EMF was carried out, which allows to fully complete the creation of a numerical design of experiments.

References

[1] Z. Xia, R. Huang, Z. Chen, K. Yu, Z. Zhang, J. R. Salas-Avila, W. Yin, Eddy current measurement for planar structures, Sensors, 22(22) (2022), 8695. doi:10.3390/s22228695.

[2] M. Lu, X. Meng, R. Huang, L. Chen, A. Peyton, W. Yin, Measuring lift-off distance and electromagnetic property of metal using dual-frequency linearity feature, IEEE Transactions on Instrumentation and Measurement, 70 (2020), doi:1-9. 10.1109/TIM.2020.3029348.

[3] M. Lu, X. Meng, L. Chen, R. Huang, W. Yin, A. Peyton, Measurement of ferromagnetic slabs permeability based on a novel planar triple-coil sensor, IEEE Sensors Journal, 20(6) (2019), 2904-2910. doi:10.1109/JSEN.2019.2957212.

[4] S. Deng, S. Yang, Y. Yao, Numerical Simulation on Stress Measurement with Eddy Current Thermography, In Electromagnetic Non-Destructive Evaluation, XXIII (2020), 97-104. doi:10.3233/SAEM200018.

[5] G. Tytko, Eddy current testing of small radius conductive cylinders with the employment of an I-core sensor, Measurement, 186 (2021), 110219. doi:10.1016/j.measurement.2021.110219.

[6] J. Burkhardt, Determination of the conductivity and thickness of conductive layers on conductive base materials, Advances in Mechanical Engineering, 11(7) (2019), 1687814019854234. doi:10.1177/168781401985423.

[7] A. Sardellitti, G. Di Capua, M. Laracca, A. Tamburrino, S. Ventre, L. Ferrigno, A fast ECT measurement method for the thickness of metallic plates, IEEE Transactions on Instrumentation and Measurement, 71 (2022), 1-12. doi:10.1109/TIM.2022.3188029.

[8] S. H. Park, J. Antony, Robust design for quality engineering and six sigma. World Scientific. 2008.

[9] S. Mukherjee, D. Kumar, L. Udpa, Y. Deng, Robust defect detection under uncertainties using spatially adaptive capacitive imaging, Journal of Applied Physics, 131(23) (2022). doi:10.1063/5.0088320.

[10] K. Krishnaiah, P. Shahabudeen, Applied design of experiments and Taguchi methods. PHI Learning Pvt. Ltd. 2012.

[11] Z. Zeng, L. Udpa, S. Udpa, Robust design of a natural gas transmission pipeline inspection tool using the Taguchi method, Research in Nondestructive Evaluation, 17(1) (2006), 17-28. doi:10.1080/09349840600582076.

[12] J. Xie, Y. Qiao, Y. Qi, Q. Xu, K. Shemtov-Yona, P. Chen, D. Rittel, Application of the Taguchi method to areal roughness-based surface topography control by waterjet treatments, Applied Surface Science Advances, 19 (2024), 100548, doi:10.1016/j.apsadv.2023.100548.

[13] A. Puška, I. Stojanović, Application of Taguchi Method in Optimization of the Extraction Procedure of Sheet Metal, Advanced Engineering Letters, 3(1) (2024), 13-20. doi:10.46793/adeletters.2024.3.1.2.

[14] T. Orosz, A. Rassõlkin, A. Kallaste, P. Arsénio, D. Pánek, J. Kaska, P. Karban, Robust Design Optimization and Emerging Technologies for Electrical Machines: Challenges and Open Problems, Applied Sciences, 10(19) 2020, 6653. doi:10.3390/app10196653.
[15] V. S. Sobolev, Y. M. Shkarlet, Surface and Screen Sensors [in Russian]. 1967.
[16] F. C. Wu, Simultaneous optimization of robust design with quantitative and ordinal data. International journal of industrial engineering: Theory, applications and practice, 15(2) (2008), 231-8. doi:10.23055/ijietap.2008.15.2.124.
[17] S. Hernández, J. Díaz, An application of Taguchi's method to robust design of aircraft structures. High Performance Structures and Materials VI, 124 2012, 3-12. doi:10.2495/HPSM120011.
[18] V. Y. Halchenko, R. V. Trembovetska, V. V. Tychkov, Development of excitation structure RBF-metamodels of moving concentric eddy current probe, Electrical Engineering & Electromechanics, (2) 2019. 28–38. doi:10.20998/2074-272X.2019.2.05
[19] V. Y. Halchenko, R. Trembovetska, V. Tychkov, Surrogate synthesis of frame eddy current probes with uniform sensitivity in the testing zone, Metrology and measurement systems, 28(3) 2021, 551-564. doi:10.24425/mms.2021.137128.